

# ‘That looks weird’ — evaluating citizen scientists’ ability to detect unusual features in ATLAS images of collisions at the Large Hadron Collider

A.J Barr<sup>a</sup>, A. Haas<sup>b</sup>, and C.W. Kalderon<sup>a,c</sup>

<sup>a</sup>Department of Physics, University of Oxford, Oxford, UK

<sup>b</sup>Department of Physics, NYU, New York, USA

<sup>c</sup>Department of Physics, University of Lund, Sweden

November 2, 2017

## Abstract

Using data from the `Higgs Hunters .org` project we investigate the ability of non-expert citizen scientists to identify long-lived particles, and other unusual features, in images of LHC collisions recorded by the ATLAS experiment. More than 32,000 volunteers from 179 countries participated, classifying 1,200,000 features of interest on about 39,000 distinct images. We find that the non-expert volunteers are capable of identifying the decays of long-lived particles with an efficiency and fake-rate comparable to that of the ATLAS algorithms. Volunteers also picked out events with unexpected features, including what appeared to be an event containing a jet of muons. A survey of volunteers indicates a high level of scientific engagement and an appetite for further LHC-related citizen science projects.

## 1 Introduction

The Large Hadron Collider is arguably the highest profile scientific project of our time. The discovery of the Higgs boson [1,2] has been the scientific highlight to date. The accelerator continues to be the subject of much media attention as searches for other new particles continue.

Matching this cutting edge science with the public’s curiosity to understand it can present a challenge. The particles themselves are invisible.

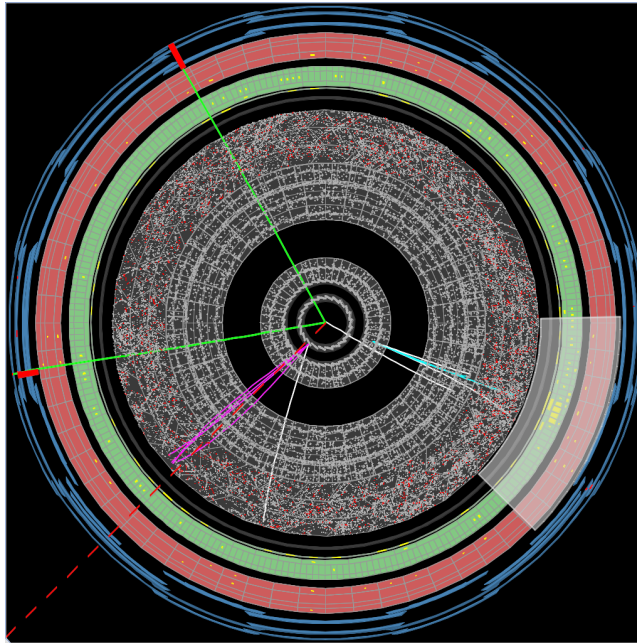


Figure 1: An example ATLAS detector image presented to citizen scientists. This image contains two off-centre vertices, each visible as a vee-like structure, at about 4 o'clock and 7 o'clock, a little distance from the center of the image. The image was generated from a computer simulation of the process  $H \rightarrow \phi + \phi$ . The green lines emanating from the centre indicate the reconstructed muon and antimuon used to select the event. The red dotted line indicates the direction of the missing momentum transverse to the beam.

Most decay a tiny fraction of a second after their creation, and can only be detected and reconstructed using large dedicated detectors assembled over decades by large international collaborations.

Despite these difficulties, there is a strong drive within science policy to get the public more involved in not just reading about science, but actually performing it. Citizen science projects – which directly involve the public in the scientific process – represent an ideal vehicle for meaningful engagement with a large community.

Non-expert citizen scientists have previously been shown to be good classifiers of images [3]. They are also capable of spotting unusual objects in images including unexpected galaxy features [4]. Through the Galaxy Zoo [5] project alone, citizen scientists have contributed to the results of 48 scientific papers [3]. The present study evaluates the extent to which analysis by non-expert citizen scientists might also be possible at the LHC.

Previously the public has been invited to contribute to CERN’s science by donating idle time on their computer to help simulate proton-proton collisions [6, 7]. This helps the scientific endeavour but with the caveat that the individual member of the public is effectively more of a provider of computing resource than an active researcher. More direct involvement in the research has previously been restricted to the relatively small fraction of the public that has a high level of computing coding skills. Such individuals have been able to directly analyse data from the ATLAS, CMS, LHCb and ALICE experiments via the CERN opendata portal [8]. The Kaggle project [9] in which members of the public were challenged to use machine learning to identify Higgs boson events also demanded a high level of coding expertise.

The HiggsHunters project is, to the best of our knowledge, the first to allow the non-expert general public a direct role in searching for new particles at the LHC. Though new in this context, it is revival of a long-established technique – before the invention of electronic particle detectors eye-scanning images of particle tracks by trained technicians was the standard analysis method.

## 2 Physics model and classification task

For the HiggsHunters.org project, a task was required which lent itself well to the strengths of non-expert citizen scientists – in particular their abilities to classify images, and to spot unusual features. The task selected was that of identifying new particles  $\phi$  — our ‘target’ bosons — as they decay within the ATLAS detector [10]. Such particles are predicted in theories in which an additional scalar mixes weakly with the Standard

### Target bosons

The theories of most interest to us predict the existence of new particles  $\phi$  which are not in the Standard Model and which have not yet been observed experimentally. In such theories the usual Higgs boson  $H$ , after it is created, would most often decay as predicted by the Standard Model, however a fraction of the time it would decay into the new particles:

$$H \rightarrow \phi + \phi.$$

The new particles  $\phi$  interact with the Standard Model only very weakly. This weak coupling means they have a slow decay rate, and hence a relatively long lifetime on the particle scale – typically of order nanoseconds. They can therefore travel a macroscopic distance, perhaps tens of centimetres, before themselves decaying.

Model Higgs boson [11].

The selected processes therefore generate a signature that is fairly easily identifiable by eye (figure 1), and which citizen scientists might therefore be competitive with a standard reconstruction algorithm. The fact that no  $\phi$  boson had been observed to date was also a very desirable feature. Unambiguous observation of evidence for these new particles would be a very significant scientific discovery, comparable to that of the discovery of the Higgs boson itself. The high impact of a potential discovery meets the important motivating feature of citizen science projects that the volunteers have a real opportunity of discovering something previously unknown to science.

## 3 Image selection

The ATLAS experiment [10] is positioned at one of the four interaction points in the LHC. It comprises a central tracking detector, surrounded by electromagnetic and hadronic calorimeters, which are themselves surrounded by a dedicated muon detector. Within the inner tracking detector, the paths of charge particles are bent by the field from a superconducting solenoidal magnet. A separate system of magnets provides a toroidal field within the muon detector.

The Large Hadron Collider provides twenty million proton-proton bunch crossings per second, far more than is practical for ATLAS to record. To

### Decay modes

The most likely decay mode of the new  $\phi$  boson depends on its mass  $m_\phi$ . If  $m_\phi$  is at least twice the mass of the  $b$  quark, the target boson will mostly decay to a bottom quark  $b$  and its anti-particle  $\bar{b}$

$$\phi \rightarrow b + \bar{b}.$$

If the mass is smaller, lying in the range  $2m_\tau < m_\phi < 2m_b$ , then the dominant decay is to a  $\tau$  lepton and its anti-particle

$$\phi \rightarrow \tau^+ + \tau^-,$$

where  $m_\tau$  and  $m_b$  are the mass of the  $\tau$  lepton and the  $b$  quark respectively. The  $\tau$  leptons and  $b$  quarks themselves have rather short lifetimes – and decay in of order picoseconds typically to many charged particles, each of which will leave a distinctive track in the ATLAS detector.

reduce the data volume, the ATLAS trigger algorithms [12] select up to several hundred of those events each second having identified features of interest such as muons, electrons, or high energy jets of hadrons.

Further selection was required before presenting images to volunteers. Given the anticipated number of volunteers (of the order of  $10^4$  to  $10^5$ ) the likely number of classifications per volunteer (anticipated to be on average ten but with a long tail of enthusiastic classifiers) and the required level of redundant classification to allow for robust analysis the desired number of images was in the range  $10^4$  to  $10^5$  events.

It was possible to select the required number of events, and simultaneously enrich them in events likely to contain Higgs bosons, by pre-selecting those events containing a muon and an antimuon with invariant mass consistent the mass of the  $Z$  boson. Such events are consistent with the  $Z$  boson decay process  $Z \rightarrow \mu^+ + \mu^-$ . Events containing a  $Z$  boson have an increased probability of also containing a Higgs boson, because virtual  $Z$  bosons may emit Higgs boson through the process  $Z^* \rightarrow Z + H$  known as ‘Higgs-strahlung’.

ATLAS uses a right-handed coordinate system with its origin at the nominal interaction point (IP) in the centre of the detector and the  $z$ -axis along the beam pipe. The  $x$ -axis points from the IP to the centre of the LHC ring, and the  $y$ -axis points upward. Cylindrical coordinates  $(r, \phi)$

are used in the transverse plane,  $\phi$  being the azimuthal angle around the  $z$ -axis. The pseudorapidity is defined in terms of the polar angle  $\theta$  as  $\eta = -\ln \tan(\theta/2)$ .

To enrich the data sample in Higgs-strahlung events over  $Z \rightarrow \mu^+ + \mu^-$  alone, the reconstructed  $Z$  boson was required to have a transverse momentum,  $p_T$ , greater than 60 GeV, a criterion which retains about 60% of the  $Z+H$  events but just 5% of the  $Z$ +jets background. A further 50% of the  $Z$ +jets background is removed through requiring that the missing transverse momentum be larger than 40 GeV. This requirement enhances the signal-to-background ratio, since the  $b$ -quark and  $\tau$ -lepton decays in the signal events often lead to a transverse momentum imbalance.

Data were selected from the 2012 data-taking period, during the period April to December, during which time the LHC was colliding protons against protons at a centre-of-mass energy of 8TeV. The data set selected corresponds to an integrated luminosity of about  $12 \text{ fb}^{-1}$ , and results in approximately 60,000 candidate  $Z \rightarrow \mu^+ + \mu^-$  events of which around 60 are expected to feature a Higgs boson.

The ability of volunteers to identify the off-centre vertices was calibrated using test images which showed Monte Carlo simulations of the process  $H \rightarrow \phi + \phi$  of interest.

Several different  $\phi$  boson masses  $m_\phi$  and average lifetimes  $\tau_\phi$  were investigated. A summary of the different processes considered can be found in table 1.

Since we are looking for decays away from the proton-proton interactions, an interesting question is the average distance which the  $\phi$  bosons can be expected to travel. The distance can be calculated using a standard relativistic calculation. The  $\phi$  boson's average lifetime in its own rest frame is  $\tau_\phi$ . Different lifetimes were selected by choosing values of  $c\tau_\phi$  where  $c$  is the speed of light. When moving at speed  $\beta$  relative to  $c$  the lifetime of the  $\phi$  boson will be increased (time dilated) by the relativistic Lorentz factor

$$\gamma = \frac{1}{\sqrt{1 - \beta^2}},$$

meaning that the average distance travelled will be  $\beta c \gamma \tau_\phi$ .

The speed of the  $\phi$  boson in the rest frame of the Higgs boson can also be calculated, this time using a relativistic energy calculation. The energy available in the Higgs boson rest frame is  $m_H c^2$  so the energy of each  $\phi$  boson from its decay is  $m_H c^2 / 2$ . Since the energy of the  $\phi$  bosons is given by  $\gamma m_\phi c^2$ , the Lorentz gamma factor in that frame is given by

$$\gamma = \frac{m_H}{2m_\phi}.$$

Thus we can calculate  $\gamma$ ,  $\beta$  can be calculated from the definition of  $\gamma$  and

Process	$\phi$ particle properties (where relevant)				Events $\geq 3$ views	
	mass $m_\phi$	$\phi$ decays to	$c\tau_\phi$	flight distance $\gamma\beta c\tau_\phi$		
$Z + H$	8 GeV	$\tau^+ + \tau^-$	1 mm	7.7 mm	3103	605
$Z + H$	8 GeV	$\tau^+ + \tau^-$	10 mm	77 mm	3119	988
$Z + H$	8 GeV	$\tau^+ + \tau^-$	100 mm	770 mm	1277	197
$Z + H$	20 GeV	$b + \bar{b}$	1 mm	3.0 mm	3012	1240
$Z + H$	20 GeV	$b + \bar{b}$	10 mm	30 mm	3094	1962
$Z + H$	20 GeV	$b + \bar{b}$	100 mm	300 mm	1341	485
$Z + H$	50 GeV	$b + \bar{b}$	1 mm	0.75 mm	2954	1183
$Z + H$	50 GeV	$b + \bar{b}$	10 mm	7.5 mm	3121	1894
$Z + H$	50 GeV	$b + \bar{b}$	100 mm	75 mm	1294	663
$Z \rightarrow \mu\mu$			—		374	321
Data			—		62278	13955
Data (debug)			—		207	178
<b>Total</b>			—		<b>85174</b>	<b>23522</b>

Table 1: Properties of the simulated images. The flight distance  $\gamma\beta c\tau_\phi$  is that for  $\phi$  particles produced from an at-rest Higgs boson, i.e. with a total energy of  $m_H/2$ . The column headed “ $\geq 3$  views” is the number of events that have had at least three citizen scientists interact with them for each of the three image projections. Where a citizen scientist examines an image but does not click, this is not counted in the above. ATLAS data were sourced from two different streams – the usual physics stream, and the ‘debug’ stream which contains events that caused problems during reconstruction.

from them find the expected distance  $\beta\gamma c\tau_\phi$  travelled by the  $\phi$  bosons in the Higgs boson rest frame, also shown in table 1. The  $\phi$  boson lifetimes have been selected such that the average distances are in the order of millimetres to metres.

All images, whether simulation or data, were processed using the ATLAS reconstruction software [13], with some additions as in Ref. [14]. The most important features of that reconstruction for this purpose are the tracks in the inner detector from the interactions of charged particles with detector elements.

For each event processed, three images are produced. Two of these are in the transverse plane perpendicular to the beam pipe, with one giving a full-detector view (**XY**) and the other a view only of the inner tracking subdetectors (**XYzoom**). The former allows for identification of ‘weird’ features in events, while the latter provides a close-up of the part most relevant for the identification of off-centre vertices. In addition to these views, there is an additional zoomed-in view showing a projection along the beam pipe (**RZzoom**), in principle allowing information in all three dimensions. All images have the central parts of the detector magnified using a fisheye projection (see Appendix) in order to better see tracks and off-centre vertices.

As of October 2016 classifications had been performed by 32,288 citizen scientists, of whom 9,610 had created Zooniverse accounts. New users are invited to create a Zooniverse account after their first five classifications, and periodically thereafter. For those classifications made without Zooniverse accounts it is assumed that classifications from different IP addresses are distinct scientists, since without an account there is no way to correct for the same individual classifying from different devices.

## 4 Evaluation of Off-Centre Vertex Identification

The question to be addressed is how effective the citizen scientists are at locating vertices. Their performance can be compared against computer algorithms that were developed and used by the ATLAS collaboration to identify off-centre vertices [14], using images in which decays of new  $\phi$  bosons have been simulated in  $H \rightarrow \phi + \phi$  decays. There are two key indicators of performance: the rate at which volunteers correctly identify the off-centre vertices and the rate at which they incorrectly identify off-centre vertices that are not from such decays – i.e. they are either image artefacts or result from some other (known and understood) process.



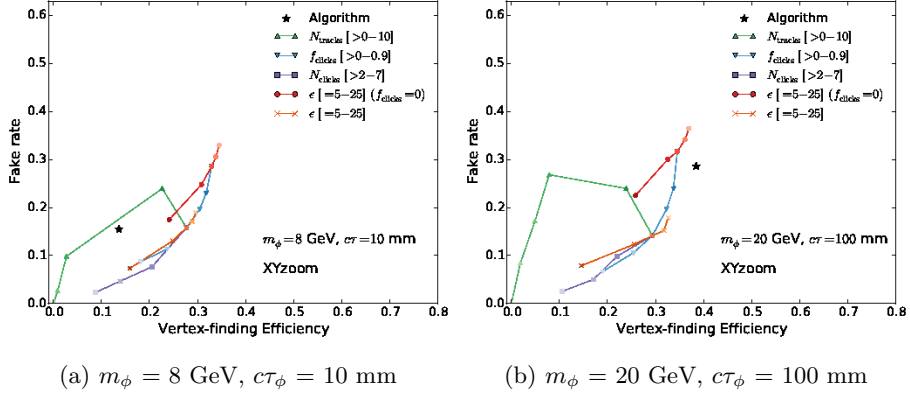


Figure 2: Example parameter choices for a selection of simulation types, both in the XY view.

Following common Zooniverse practice, each event is classified by  $\sim 60$  people, translating to  $\sim 20$  per image (three projections per image) – including ‘classifications’ where no image features were marked. In what follows, only images where at least three citizen scientists have marked an off-centre vertex are considered.

To aggregate classifications across citizen scientists, the DBSCAN clustering algorithm [15] was used to find clusters of clicks. It requires a clustering size parameter,  $\epsilon$ , in addition to the 2D co-ordinates of click positions. Further selections were imposed on the cluster candidates, requiring them to be formed of at least  $N_{\text{clicks}}$  individual clicks, to have contributions from at least a fraction  $f_{\text{clicks}}$  of people who marked a vertex on the image, and to be formed only from clicks where the vertex has been identified by the citizen scientist as featuring at least  $N_{\text{tracks}}$  tracks (which can be zero in the case that no number was provided by a citizen scientist). Once a parameter choice has been made and a set of clusters formed for each image, the refined clusters are compared to the known decay positions of the  $\phi$  particles in the simulation. If a cluster is closer than 25 pixels (images are  $1024 \times 1024$  pixels) to the nearest decay position, it is considered to be a correct identification and both cluster and true decay position are removed from consideration, before repeating the matching for remaining clusters. Any cluster not matched to a true decay position in this way is considered a ‘fake’ cluster. Then the efficiency is  $\sum_{N_{\text{events}}} N_{\text{matched clusters}} / 2 \times N_{\text{events}}$  and the fake rate is  $\sum_{N_{\text{events}}} N_{\text{unmatched clusters}} / N_{\text{events}}$ , since there are two true vertices per image.

Figure 2 shows some examples of how these parameter choices can affect the resulting efficiency and fake rate. A baseline choice is taken as  $\epsilon = 15$ ,  $N_{\text{tracks}} \geq 0$ ,  $N_{\text{clicks}} \geq 3$ ,  $f_{\text{clicks}} \geq 0.7$ , striking a balance between high efficiency and low fake rate. As a measure comparing the vertices from the reconstruction algorithm and citizen scientists' click clusters, the efficiencies for each are shown in table 2, with clustering parameters chosen so as to give the same fake rate for both.

It can be seen that some  $\phi$  parameter sets fare worse, some better and some similarly (e.g. both a lower fake rate and efficiency), indicating that the citizen scientists are in many cases outperforming the reconstruction.

Table 2 shows a comparison between the algorithm's efficiency and that of the citizen scientists for the different masses and lifetimes of the target boson  $\phi$ .

Since the parameters of the clustering algorithm can be varied to increase vertex-finding efficiency as the cost of increasing the number of fakes, the efficiency for the citizen scientist clustering is taken as the maximal efficiency which gives the same fake rate as obtained by the algorithm. This is the rightmost intercept of the coloured lines and a horizontal one through the star in figure 2. Where no such intercept exists because the algorithm always has a higher fake rate than the citizen scientists for all clustering parameters, the efficiency for the citizen scientists is taken to be that with the highest fake rate found, and shown as a lower bound. This is a conservative estimate of their efficiency since it is known that the citizen scientists can achieve at least this efficiency even at a lower fake rate.

The efficiencies and fake rates differ between views since some vertices fall outside the image boundaries and are not counted towards the calculations, and not all events have been examined by at least three people in all three views (so the set of events considered differs slightly between views). In general the citizen scientists had more difficulty locating the vertices in the **RZzoom** view. This was expected by the experimenters, nevertheless the view was included since it offers the possibility of three-dimensional vertex reconstruction.

Overall it can be seen that the performance of the citizen scientists competes very well with that of the computer algorithm. The collective ability of the citizen scientists tends to beat the computer algorithm for simulations with low mass (8 GeV) target bosons. This is true for almost all views and all tested values of the lifetimes. As the mass of the boson  $\phi$  increases the citizen scientists generally retain a very respectable efficiency, but the balance shifts in favour of the algorithm.

It's interesting to speculate on why the relative performance of the





































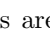
$\phi$ properties		View	Fake rate [%]	Efficiency [%]		Winner
$m$ [GeV]	$c\tau_\phi$ [mm]					
8	100	XY	14	8	14	
8	100	XYzoom	13	7	12	
8	100	RZzoom	12	6	4	
8	10	XY	15	15	27	
8	10	XYzoom	15	14	29	
8	10	RZzoom	12	13	9	
8	1	XY	22	8	9	 / 
8	1	XYzoom	21	7	11	
8	1	RZzoom	16	5	5	 / 
20	100	XY	27	39	37	 / 
20	100	XYzoom	29	38	34	 / 
20	100	RZzoom	27	33	21	
20	10	XY	40	59	$\geq 47$	 / 
20	10	XYzoom	44	57	$\geq 52$	 / 
20	10	RZzoom	40	56	$\geq 34$	
20	1	XY	26	36	11	
20	1	XYzoom	31	34	17	
20	1	RZzoom	27	34	12	
50	100	XY	41	59	$\geq 46$	 / 
50	100	XYzoom	43	59	$\geq 48$	 / 
50	100	RZzoom	39	57	$\geq 32$	
50	10	XY	51	72	$\geq 35$	
50	10	XYzoom	53	70	$\geq 41$	
50	10	RZzoom	50	69	$\geq 28$	
50	1	XY	27	41	9	
50	1	XYzoom	31	40	6	
50	1	RZzoom	28	40	6	

Table 2: Vertex-finding efficiencies for citizen scientists (marked with an eye) and the computer algorithm (marked with computer). Efficiencies are shown for each of the mass and lifetime of the target boson  $\phi$  and for the three views considered. The symbols in the final column are an eye where citizen scientists outperform the algorithm, and a computer where the algorithm outperforms. Where the losing strategy achieves an efficiency of at least 75% of the winning one (i.e the result is marginal) its symbol follows that of the winner. When the fake rate of the algorithm is always higher than that of the citizen scientists for any set of clustering parameters then only a lower bound can be placed on the eye efficiency value that would be found for equal fake rates.

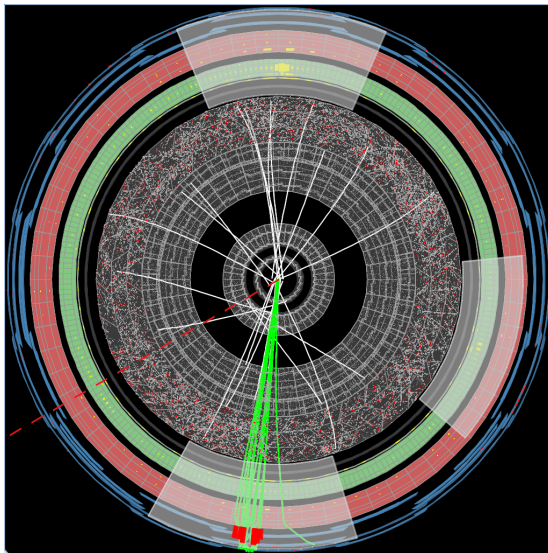


Figure 3: The original ‘muon jet’ image, identified by a user on 27th November 2014. There appear to be a large number of muons (green lines passing all the way through the detector) all very close together.

algorithm versus the eye depends on the mass of the target boson. One reason may be that heavier  $\phi$  particles have lower velocities  $\beta$ , and hence lower Lorentz factors  $\gamma$  in the Higgs boson rest frame. This decreases their travel distance  $\beta\gamma c\tau_\phi$  for any particular  $\tau_\phi$ . Another factor might be that the heavier  $\phi$  particles decay to  $b + \bar{b}$  quarks rather than to  $\tau^+ + \tau^-$  leptons as is the case for the lighter  $\phi$  bosons.

## 5 The ‘Muon-Jet’ Event

In addition to being able to mark off-centre vertices, the citizen scientists are also encouraged to select anything ‘weird’ in the images, and to follow up these on the ‘talk’ forum [16] where the wider community discusses them. This raised several instances of known phenomena, such as cosmic ray showers passing through ATLAS, but also some that were unexpected.

Some such oddities were particularly surprising. Soon after the project’s launch, the image in figure 3 was flagged as weird and posted in the talk forum by several citizen scientists. The image shows a collision apparently containing a jet of multiple collimated muons. Such a feature is not expected in the Standard Model of particle physics, where jets are always of hadrons, not of muons. The observations caused a flurry of activity

amongst both the citizen scientists and the science team.

After further investigation by the science team, it was revealed that this event was an example of ‘punch-through. This is an unusual interaction of a known particle with the detector, rather than an unusual or new particle. So while it does not represent a discovery of new physics, this example clearly shows the potential for untrained citizen scientists to isolate interesting features in real LHC collision data.

## 6 Conclusion

The first mass participation citizen science project for the Large Hadron Collider has been extremely successful. More than 32,000 citizen scientists participated, and more than 1.2 million features of interest were identified in images from the ATLAS detector.

The collective ability of the citizen scientists was found to be very high. They were effective at locating secondary vertices of long-lived particles, with efficiency and false-identification rates competitive with (and in some cases better than) the ATLAS reconstruction algorithms.

Amongst the unusual features volunteers spotted were what appeared to be jets of muons, features unexpected in the Standard Model of particle physics, and which later analysis showed to be a feature known as calorimeter punch-through.

## Acknowledgements

The `HiggsHunters.org` project is a collaboration between the University of Oxford and the University of Birmingham in the United Kingdom, and NYU in the United States. It makes use of the Zooniverse citizen science platform, which hosts over 40 projects from searches for new astrophysical objects in telescope surveys to following the habits of wildlife in the Serengeti. The HiggsHunters project shows collisions recorded by the ATLAS experiment and uses software and display tools developed by the ATLAS collaboration. The authors gratefully acknowledge the generous financial support of the UK Science and Technology Facilities Council, the University of Oxford, and Merton College, Oxford.

The data used in this work is available upon request from the Institute for Research in Schools [17].

# Appendix

## A Simulation and image reconstruction details

Calibration  $Z(\rightarrow \mu^+\mu^-)+H(\rightarrow \phi\phi)$  events were generated using `MadGraph-5.1.5.2` [18] interfaced to `Pythia-8.175` [19, 20] using the `AU2` tune [21] of `Pythia` parameters with the `CTEQ6L1` [22] PDF set. The  $\phi$  is a pseudoscalar boson, i.e. a spinless particle with negative parity.

They were passed through ATLAS simulation infrastructure [13], and simulated pileup events from the same and surrounding bunch crossings were added, along with modelled detector noise, corresponding to the same luminosity profile as the 2012 data sample.

Tracks and vertices were reconstructed as described in Ref. [14]. In particular, the tracking was extended from the ATLAS default impact parameter of 1 cm, to 10 cm. The total simulation and reconstruction time was about 10 minutes per event, or  $\sim 1$  CPU-year. (This was spread out to many computers on the ATLAS grid to process  $\sim 50$ k events in  $\sim 2$  days.)

The total data size of  $\sim 250$  GB was then reduced to  $\sim 100$  GB of images. These images were made using the ATLAS Atlantis event display [23, 24]. Selections were applied to reduce the amount of visual information (clutter) shown in each image, while still allowing vertices to be seen. Only tracks with  $p_T > 2$  GeV and starting  $> 0.5$  mm in the transverse plane from the beamline were shown (since there are  $\sim 1000$ 's of low  $p_T$ , tracks originating from the interaction point.) Tracks that start more than 20 cm from the center of the detector or the selected collision point in the direction along the beamline are not drawn. To reduce the number of fake tracks, they must have at least seven hits in the silicon strip tracker. Vertices shown must have at least three tracks. Muon tracks must have  $p_T > 10$  GeV, and jets of hadrons must have  $p_T > 40$  GeV. Other objects (photons, electrons, bottom quark jets, etc.) are drawn as long as they have  $p_T > 5$  GeV.

The images were displayed using a non-linear radially dependent fish-eye transform of the form

$$r' = \frac{ar}{m(1+cr)}$$

where  $a$ ,  $c$  and  $m$  are real positive constants, and  $r$  is the radius in pixels in the  $x-y$  view. This transform serves to increase viewers' attention to and precision within the central tracking layers of the ATLAS detector.

## References

- [1] ATLAS Collaboration. Observation of a new particle in the search for the Standard Model Higgs boson with the ATLAS detector at the LHC. *Phys Lett B*. 2012;716:1.
- [2] CMS Collaboration. Observation of a new boson at a mass of 125 GeV with the CMS experiment at the LHC. *Phys Lett B*. 2012;716:30.
- [3] Zooniverse collaboration; 2016. The Zooniverse project: publications. Available from: <https://www.zooniverse.org/about/publications>.
- [4] Lintott CJ, Schawinski K, Keel W, Van Arkel H, Bennert N, Edmondson E, et al. Galaxy Zoo: Hanny's Voorwerp, a quasar light echo? *Monthly Notices of the Royal Astronomical Society*. 2009;399(1):129–140.
- [5] Zooniverse collaboration; 2007. Galaxy Zoo project. Available from: <https://www.galaxyzoo.org/>.
- [6] Purcell A; 2004. LHC@home. Available from: <http://lhcatome.web.cern.ch/>.
- [7] ATLAS collaboration; 2014. ATLAS@HOME. Available from: <http://atlasathome.cern.ch/>.
- [8] CERN; 2014. CERN open data. Available from: <http://opendata.cern.ch>.
- [9] ATLAS Collaboration; 2014. Higgs Boson Machine Learning Challenge. Available from: <https://www.kaggle.com/c/higgs-boson>.
- [10] ATLAS Collaboration. The ATLAS Experiment at the CERN Large Hadron Collider. *JINST*. 2008;3:S08003.
- [11] Strassler MJ, Zurek KM. Discovering the Higgs through highly-displaced vertices. *Phys Lett B*. 2008;661:263–267.
- [12] ATLAS Collaboration. Performance of the ATLAS Trigger System in 2010. *Eur Phys J C*. 2012;72:1849.
- [13] ATLAS Collaboration. The ATLAS Simulation Infrastructure. *Eur Phys J C*. 2010;70:823.
- [14] ATLAS Collaboration. Search for massive, long-lived particles using multitrack displaced vertices or displaced lepton pairs in pp collisions at  $\sqrt{s} = 8$  TeV with the ATLAS detector. *Phys Rev D*. 2015;92(7):072004.
- [15] Ester M, Kriegel HP, Sander J, Xu X. A density-based algorithm for discovering clusters in large spatial databases with noise. AAAI

Press, Proceedings of the Second International Conference on Knowledge Discovery and Data Mining (KDD-96). 1996;p. 226. Available from: <http://citeseerx.ist.psu.edu/viewdoc/summary?doi=10.1.1.121.9220>.

- [16] HiggsHunters collaboration; 2014. <https://talk.higgshunters.org>.
- [17] Institute for Research in Schools; 2016. [http://www.researchinschools.org/higgs\\_hunters](http://www.researchinschools.org/higgs_hunters).
- [18] Alwall J, Herquet M, Maltoni F, Mattelaer O, Stelzer T. MadGraph 5 : Going Beyond. JHEP. 2011;06:128.
- [19] Sjöstrand T, Mrenna S, Skands PZ. PYTHIA 6.4 Physics and Manual. JHEP. 2006;05:026.
- [20] Sjöstrand T, Mrenna S, Skands PZ. A Brief Introduction to PYTHIA 8.1. Comput Phys Commun. 2008;178:852.
- [21] ATLAS Collaboration. Summary of ATLAS Pythia 8 tunes. ATL-PHYS-PUB-2012-003;Available from: <https://cds.cern.ch/record/1474107>.
- [22] Pumplin J, et al. New generation of parton distributions with uncertainties from global QCD analysis. JHEP. 2002;07:012.
- [23] ATLAS collaboration. Atlantis – Event display for ATLAS; 2003. <http://atlantis.web.cern.ch/atlantis/>.
- [24] Taylor G. Visualizing the ATLAS Inner Detector with Atlantis. Nucl Instrum Meth. 2005;A549:183–187.